Hyperfine structure of the $4s$, $4p$, and $3d$ states in Ca^+ evaluated by many-body perturbation theory

Ann-Marie Mårtensson-Pendrill and Sten Salomonson*
Department of Physics, Chalmers University of Technology, S-412 96 Göteborg, Sweden
(Received 25 October 1983)

The hyperfine structure of the $4s$, $4p$, and $3d$ states in Ca^+ has been evaluated with the use of many-body perturbation theory. Core-polarization and correlation effects have been included by solving inhomogeneous one- and two-particle differential equations. By solving these equations iteratively, these effects have been treated also to higher orders. Certain correlation effects have been accounted for by modifying the valence orbitals to approximate "Brueckner orbitals." Relativistic effects were estimated on the basis of relativistic calculations including core polarization. The final results for ^{43}Ca are $A(4^2S_{1/2})=-819$ MHz, $A(4^2P_{1/2})=-148$ MHz, $A(4^2P_{3/2})=-30.9$ MHz, $B(4^2P_{3/2})/Q=155$ MHz/b, $A(3^2D_{3/2})=-52$ MHz, $B(3^2D_{3/2})/Q=68$ MHz/b, $A(3^2D_{5/2})=-5.2$ MHz, and $B(3^2D_{5/2})/Q=97$ MHz/b.

I. INTRODUCTION

Calcium is a commonly occurring element in systems of biological importance and its abundance can be studied by means of nuclear-magnetic-resonance methods.[1] The understanding of the relaxation processes requires a knowledge of the nuclear quadrupole moment of ^{43}Ca, which is the only naturally abundant Ca isotope with nonzero nuclear spin. The quadrupole moment can be obtained from a study of the electric hyperfine structure (hfs) in free Ca atoms, provided the electronic factors involved are known. However, the strong correlation between the two valence electrons calls for extreme care in the theoretical treatment. Calculations for the Ca atom will be presented elsewhere and we concentrate here on the study of the alkali-metal-atom-like system Ca^+, extending earlier work where extensive calculations were performed on the hyperfine structure of the alkali-metal atoms.[2–5] Results are presented for the $4s$, $4p$, and $3d$ states of Ca^+.

If a central-field model is used to describe the alkali-metal-atom-like system, the hfs is determined to lowest order by the expectation value $\langle r^{-3}\rangle$ of the valence electron (for a non-s state). However, the interaction with the valence electron disturbs the core and this perturbation influences differently the so-called contact, orbital, spin-dipole, and quadrupole $\langle r^{-3}\rangle$ parameters, commonly used to analyze experimental hfs data. Sternheimer[6] used the inhomogeneous differential equation technique to calculate the first-order core polarization contribution, from which he deduced "shielding factors" to be used in the evaluation of nuclear quadrupole moments from hfs data. His method has been extended to treat the polarization effects to all orders by means of an iterative procedure.[3] Pair correlation effects, which involve the simultaneous modification of two orbitals, have been included, as described in Ref. 2, by solving inhomogeneous two-particle equations. The double summation over large basis sets[7] is thus avoided.

Lindgren *et al.*[4] have demonstrated that certain important pair correlation effects can be taken into account by modifying the orbitals to approximate "Brueckner" orbitals. A reevaluation of the contributions with these orbitals has lead to a significant improvement of the theoretical results.[4] Further improvement has been obtained by solving also the pair equation iteratively.[5,8] The procedure used in this paper has been described in detail in earlier work and is also presented in a recent book by Lindgren and Morrison.[9] A brief summary is given in Sec. II.

In Sec. III the results obtained for the $4s$, $4p$, and $3d$ states in Ca^+ are presented. The value obtained for the $4s$ state, $A(4^2S_{1/2})=-819$ MHz, agrees well with the result -817 ± 15 MHz obtained by Kelly *et al.*[10] The $3d$ state, having lower energy than the $4p$ state, is metastable and can thus be studied, e.g., by radio-frequency spectroscopy. However, to our knowledge no experimental hyperfine-structure results are available for any of the excited states.

II. CALCULATION OF THE HYPERFINE STRUCTURE

In the nonrelativistic formalism used here, the hyperfine operator is given (in atomic units) by

$$h^{\rm hfs}=\alpha^2\left[\vec{l}\,r^{-3}-\sqrt{10}(\vec{s}\,\vec{C}^{\,2})^1 r^{-3}+\frac{2}{3}\frac{\vec{s}\,\delta(r)}{r^2}\right]\cdot\vec{\mu}_I-\tfrac{1}{2}r^{-3}\vec{C}^{\,2}\cdot\vec{Q}\,, \tag{1}$$

where $\vec{\mu}_I = g_I \mu_N \vec{I}$ is the nuclear magnetic moment and $\vec{Q}$ is the electric quadrupole moment of the nucleus. The terms in the hfs operator are referred to as orbital, spin-dipole, contact, and quadrupole terms, respectively. For systems with one valence electron, the hfs operator can be replaced by an "effective operator"

$$h_{\text{eff}}^{\text{hfs}} = \alpha^2 [\vec{l} \langle r^{-3} \rangle_{01} - \sqrt{10} (\vec{s} \vec{C}^2)^1 \langle r^{-3} \rangle_{12} + \vec{s} \langle r^{-3} \rangle_{10}] \cdot \vec{\mu}_I - \tfrac{1}{2} \vec{C}^2 \cdot \vec{Q} \langle r^{-3} \rangle_{02} \, . \tag{2}$$

In lowest-order perturbation theory, illustrated by the diagram in Fig. 1, all $\langle r^{-3} \rangle$ parameters (except the contact parameter $\langle r^{-3} \rangle_{10}$) have the same value. However, Harvey found that it is necessary to use different values to reproduce experimental data.[11] This can be explained by terms appearing in higher orders in the perturbation expansion.

A. Core-polarization contributions to the hyperfine structure

For a one-particle perturbation, like the hfs, the second-order contributions, shown in Fig. 2, involve only single-particle excitations. These can be described as "core polarization." The calculation of the effect involves the summation over all excited states including the continuum. The contribution from the exchange core-polarization diagram [Fig. 2(c)], e.g., is given by

$$-\sum_a^{\text{core}} \sum_r^{\text{exc}} \frac{\langle a,o \mid r_{12}^{-1} \mid o,r \rangle \langle r \mid h^{\text{hfs}} \mid a \rangle}{\epsilon_a - \epsilon_r} \, .$$

However, the infinite summation can be circumvented through the inhomogeneous differential equation method, first used by Sternheimer.[6] A "single-particle function"

$$\rho_a = \sum_r^{\text{exc}} \frac{|r\rangle \langle r \mid h_{\text{hfs}} \mid a \rangle}{\epsilon_a - \epsilon_r}$$

can be obtained as a solution to the inhomogeneous differential equation

$$(\epsilon_a - h_0)\rho_a = h_{\text{hfs}} \mid a \rangle - \sum_b^{\text{core}} \mid b \rangle \langle b \mid h_{\text{hfs}} \mid a \rangle \, . \tag{3}$$

The closure relation, $\sum_i^{\text{all}} \mid i \rangle \langle i \mid = 1$, has been used to remove the infinite summation over excited states on the right-hand side. The summation over all core orbitals makes the right-hand side orthogonal to the core and will hereafter be referred to as "orthogonality terms." With the use of the single-particle function ρ_a the contribution from Fig. 2(c) can simply be expressed as

$$\langle a,o \mid r_{12}^{-1} \mid o,\rho_a \rangle \, . \tag{4}$$

The inhomogeneous differential equation (3) is converted to a set of one-dimensional radial equations by separating ρ_a into parts with excitations $nl \rightarrow l'$ to a well-defined orbital angular momentum l' and by defining different single-particle functions for the different terms in the hfs operator in (1).

The perturbation of orbital a due to the hfs operator, as described by ρ_a, will in turn polarize the other orbitals through a change in the electrostatic interaction. As shown by Garpman *et al.*[3] the core-polarization effects can be treated self-consistently, "to all orders," by means of an iterative procedure. The single-particle functions ρ_b can be used to modify the right-hand side of Eq. (3) to

$$(\epsilon_a - h_0)\rho_a = h_{\text{hfs}} \mid a \rangle + \sum_b [(\langle b \mid r_{12}^{-1} \mid \rho_b \rangle + \langle \rho_b \mid r_{12}^{-1} \mid b \rangle) \mid a \rangle - (\langle b \mid r_{12}^{-1} \mid a \rangle \rho_b + \langle \rho_b \mid r_{12}^{-1} \mid a \rangle \mid b \rangle)] - \cdots \, , \tag{5}$$

where the ellipsis represents the orthogonality terms. This procedure is repeated until convergence. The recursive equation (5) can be represented by the diagrams in Fig. 3. When the single-particle functions from (5) are inserted in (4), higher-order core-polarization contributions are automatically included. This method of calculating the core-polarization effects to all orders has recently been ex-

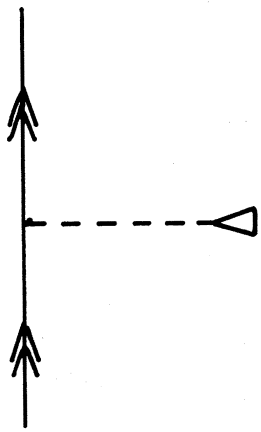

FIG. 1. First-order contribution to the hyperfine structure in diagrammatic form. The lines with double arrows represent the valence orbital and the dashed line with a triangle the hyperfine interaction.

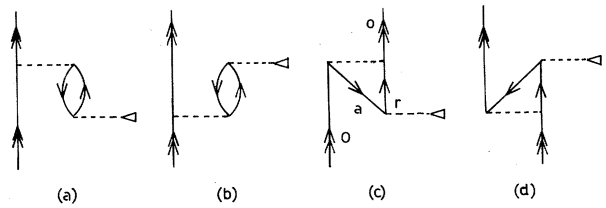

FIG. 2. Second-order (lowest-order core-polarization) contributions to the hyperfine structure. The dashed line represents the electrostatic interaction and a down- (up-) going line with one arrow represents a core (excited) orbital.

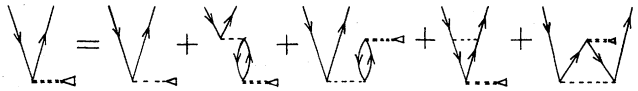

FIG. 3. Recursive relation, corresponding to Eq. (5), for the "effective" single-particle function ρ_a. The first term on the right-hand side represents the first-order single-particle function. A double dashed line with a triangle is used to represent the "effective" hyperfine interaction.

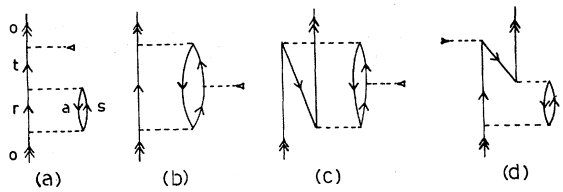

FIG. 4. Examples of third-order correlation diagrams.

tended to the relativistic case.[12] Our definition of higher-order polarization effects differs slightly from that used by Das and co-workers.[7] They exclude the so-called "consistency effects," corresponding to the terms $b \neq a$ in Eq. (5) above. Their "ladder correction" includes, however, in addition to the $a=b$ terms in Eq. (5), also higher-order interactions with the valence electron. These are treated together with the correlation effects in our calculations.

The different values of the $\langle r^{-3} \rangle$ parameters in (2) can be understood by inspection of the angular momentum restrictions on the core-polarization contributions. Only $nl \rightarrow l$, $l > 0$, excitations contribute to the orbital parameters, whereas the spin-dipole and quadrupole interactions both involve the somewhat looser restriction $|l - l'| \leq 2$, $l + l' \geq 2$. However, the spin-dipole interaction differs from the quadrupole interaction in the presence of the spin operator, which prevents the direct diagrams [Figs. 2(a) and 2(b)] from contributing. Thus all $\langle r^{-3} \rangle$ parameters involve different excitations and can take different values.

In first order the contact parameter enters only for s states. However, $ns \rightarrow s$ excitations in the core give rise to an induced contact parameter also for states with $l > 0$. In higher orders also $nl \rightarrow l$ ($l > 0$) core excitations are induced by the $ns \rightarrow s$ excitations.

B. Third-order contributions to the hyperfine structure

Although the core-polarization explains why all $\langle r^{-3} \rangle$ parameters may be different, it often fails to account for the numerical values of the hfs parameters. The discrepancies are due to correlation effects. A few of the correlation diagrams that enter in third order are shown in Fig. 4. The evaluation of the third-order diagrams has been described in Ref. 2. As an example we give here the contribution from Fig. 4(a):

$$\sum_{a}^{\text{core}} \sum_{r,s,t}^{\text{exc}} \frac{\langle o \,|\, h_{\text{hfs}} \,|\, t \rangle \langle t,a \,|\, r_{12}^{-1} \,|\, r,s \rangle \langle r,s \,|\, r_{12}^{-1} \,|\, o,a \rangle}{(\epsilon_o - \epsilon_t)(\epsilon_o + \epsilon_a - \epsilon_r - \epsilon_s)} .$$

The infinite summation over t can be obtained through the solution of the single-particle equation (3) above, whereas the double summation over the excited states r and s requires the solution of a two-particle equation

$$(\epsilon_o + \epsilon_a - h_0(1) - h_0(2)) U_{oa}(1,2) = r_{12}^{-1} \,|\, o,a \rangle - \cdots ,$$

where the ellipsis represents the orthogonality terms. The pair equation has been solved numerically by the procedure described in Ref. 8. With the use of the single-particle function ρ_o from (3) and the pair function U_{oa}, the contribution from the diagram in Fig. 4(a) can be written as

$$\langle \rho_o a \,|\, r_{12}^{-1} \,|\, U_{oa} \rangle .$$

The diagrams in Figs. 4(b) and 4(c) require two pair functions. The diagram in Fig. 4(d) is evaluated using one pair function and one single-particle function describing the excitation of one core orbital. Instead of using the first-order single-particle function described by Eq. (3), we have used the "all-order" single-particle function obtained from Eq. (5). Thus third-order diagrams like the diagram in Fig. 4(d) will implicitly include certain higher-order diagrams.

The evaluation of pair correlation effects is the most time consuming part of the calculation due to the need to describe (and solve the equation for) a two-dimensional radial function. To combine reasonable computing time with relatively good accuracy we evaluate the effects using three different grid sizes and use Richardson extrapolation to remove the $O(h^2)$ and $O(h^4)$ errors introduced by the numerical procedure.[8]

C. Correlation effects on the orbitals

Sometimes even the inclusion of all third-order contributions to the hfs fails to reproduce the experimental data. Instead of evaluating all fourth-order diagrams, we have chosen to include certain important higher-order correlation effects by modifying the orbitals. By adding to the orbital, o, a corrections, δo, which is described by Fig. 5 and satisfies the equation

$$(\epsilon_o - h_0) \,|\, \delta o \rangle = \langle a \,|\, r_{12}^{-1} \,|\, U_{oa} \rangle - \cdots , \tag{6}$$

where the ellipsis represents orthogonality terms, Fig. 4(a) is automatically included in the expectation value $\langle o + \delta o \,|\, h_{\text{hfs}} \,|\, o + \delta o \rangle$ of the hfs operator. [As shown in

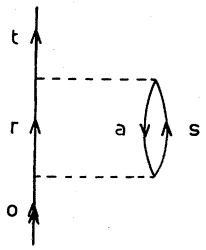

FIG. 5. Second-order correlation correction to the valence orbital described by Eq. (6). This type of correction is included in "Brueckner" valence orbitals.

in Ref. 4, a few more terms appear on the right-hand side of (6), which account for other diagrams, analogous to 4(a), which have not been shown here.]

By replacing the Hartree-Fock orbitals by these approximate "Brueckner" orbitals, not only the expectation value but also the polarization and correlation effects are modified. The lowest-order exchange polarization diagram, Fig. 2(c), e.g., will include also the fourth-order diagram shown in Fig. 6(a) and the third-order correlation diagram, Fig. 4(b), will include the fifth-order diagram in Fig. 6(b).

In the Hartree-Fock (HF) potential for the inert-gas-like core, which has been used here, the core is not affected by the valence electron. The modification, δo, of the valence orbital, described by the diagram in Fig. 5, can be interpreted as an adjustment in the valence orbital due to the change the valence electron has induced in the core. Figure 5 involves a pair excitation and only a part of the excitation to the same angular symmetry can be taken into account by using the HF potential with the valence electron included. This part is often very small and true pair excitations, especially excitations where the angular momentum is changed by one unit for each electron, dominate the modification of the orbitals to approximate Brueckner orbitals.

It can be noted that Ahmad *et al.* in recent relativistic calculations of the hyperfine structure of the ground states in Mg^+ (Ref. 13) and Ba^+ (Ref. 14) evaluated directly only correlation diagrams of the type in Fig. 4(a). For Mg^+ only $\Delta l=0$ and 1 excitations were included. The size of the remaining correlation diagrams in third order was estimated from results obtained for other systems.[7]

For the $5d$ state in K and the $4d$ state in Rb the inclusion of these orbital modifications caused a contraction of the valence orbital leading to a doubling of the $\langle r^{-3}\rangle$ expectation value.[4] In this work we have evaluated the modification of the orbitals towards approximate Brueckner orbitals only for the valence electrons.

D. Higher-order correlation effects

The modification of the orbitals to approximate Brueckner orbitals significantly improved the agreement between theory and experiment.[4] Nevertheless, some discrepancies remained. Therefore, a procedure was developed to treat pair correlation effects in a self-consistent way in analogy with the iterative procedure for core-polarization described above. The iterative procedure has been applied to the correlation energy in He,[8] and Ne,[15] and to the calculation of the hfs of s states in Na (Ref. 16) and of the $4d$ state in Rb.[5] Use of the iterated pair functions brought the desired agreement between theory and experiment for the $4d$ state in Rb.

III. RESULTS AND DISCUSSION

Of the naturally abundant calcium isotopes only ^{43}Ca, with an abundance of 0.14%, has a nonzero nuclear spin giving rise to a hyperfine structure. The spin is $I=\frac{7}{2}$ and the nuclear magnetic moment is $\mu_I=g_I I=-1.317\,642(7)$ nm.[17] This value is corrected for diamagnetic screening (a 0.15% effect). It has been used to obtain the results for ^{43}Ca given in MHz. All other results are given in Hartree atomic units (a.u.).

A. The 4s state

The ground state of Ca^+, $4s\,^2S_{1/2}$, has only a contact parameter $\langle r^{-3}\rangle_{10}$, due to the angular restrictions. It is given in first order by $\frac{2}{3}R^2_{4s}(0)=15.69$ a.u. Of course, this value is changed by higher-order contributions, as shown in Table I.

The most important correction is due to single excitations, "core polarization," which contribute 3.3. As expected the $3s\rightarrow s$ excitations dominate and contribute 2.2. The $2s\rightarrow s$ and $1s\rightarrow s$ excitations contribute 0.7 and 0.5, respectively, and the indirect contributions from $3p\rightarrow p$ and $2p\rightarrow p$ excitations are very small. Our core polarization, giving a 21% increase of the $\langle r^{-3}\rangle_{10}$ parameter, is somewhat larger than the results 14% and 19%, respectively, obtained by Ahmad *et al.* for Mg^+ (Ref. 13) and Ba^+.[14] This is probably due to the above-mentioned difference in the definition of core-polarization effects.

The modification of the valence orbital to an approximate Brueckner orbital gives a slightly smaller increase, about 18% or 2.8. Of this contribution 2.4 arises from $4s\,3p$ excitations with 1.6 from $4s\,3p\rightarrow pd$, 0.4 from $4s\,3p\rightarrow sp$, and 0.1 from $4s\,3p\rightarrow ps$. Excitations from $4s\,2p$ and $4s\,2s$ contribute about 0.2 each and excitations involving two core orbitals 0.01. This orbital modification contributed 11% of the first-order value for Mg^+

TABLE I. Various contributions to the contact parameter $\langle r^{-3}\rangle_{10}$ for the $4s$ state in Ca^+ (a.u.).

	$\frac{2}{3}R^2_{4s}(0)$	Polarization	Correlation	Total
Hartree-Fock (Ca^{2+} core) "Brueckner orbitals"	15.69	3.28	2.42[a]	21.39
Pair functions used:				
First order	18.52	3.69	−0.44	21.77
1 iteration	18.51	3.71	−0.38	21.84
2 iterations	18.53	3.71	−0.38	21.86
3 iterations	18.53	3.71	−0.38	21.86

[a] 2.78 of this value can be ascribed to the correction of the valence orbital to an approximate Brueckner orbital and the rest, −0.36, arising from other correlation effects is the number to be compared to the other values in the column.

(Ref. 13) and 30% for Ba^+,[14] showing that its relative importance increases with the nuclear charge. The contraction of the $4s$ electron orbital also causes the core-polarization contribution to increase by about 13%, thus increasing the first-order value by 2.7%.

The remaining correlation effects are very small (2.4% of the first-order value) and, as could be expected from this observation, very little is gained in this case by including higher-order correlation effects. The total nonrelativistic result corresponds to an A factor of -785 MHz.

The radial pair functions used to calculate the modification of the valence orbital towards an approximate Brueckner orbital and the remaining correlation effects, were obtained in three different grid sizes [59, 69, and 79 points, respectively, in the range exp(−7.1) to exp(4.1)] and grid extrapolation was applied to remove the $O(h^2)$ and $O(h^4)$ errors.

Table II shows the pair excitations included in the calculation. All excitations from two core electrons to excited states involving at least one s, p, or d electron were included. Excitations, where the l values were changed up to 4 units were allowed for valence-core pair excitations. All excitations involving a $1s$ electron have been neglected. No extrapolation was performed to estimate the contributions from higher l values.

Use of relativistic Dirac-Fock orbitals instead of nonrelativistic Hartree-Fock orbitals increases both the first-order $\langle r^{-3}\rangle$ value and the core-polarization contributions by about 4.4% to 16.38 and 3.42, respectively. Adding the nonrelativistic correlation contribution to these results gives an A factor of -815 MHz. If 4.4% are added to the correlation contribution as an estimate of the relativistic effects, a final result of -819 MHz is obtained. The value can be compared to the semiempirical result, -827 MHz (Ref. 18) obtained from the Fermi-Segrè-Goudsmit formula,[19] and agrees well with the experimental result of -817 ± 15 MHz obtained by Kelly *et al.*[10]

TABLE II. List of pair excitations included in the calculations.

core-core	$3p^2\rightarrow s^2,\ p^2,\ d^2,\ sd,\ pf,\ dg$
	$3p\,2p\rightarrow s^2,\ p^2,\ d^2,\ sd,\ ds,\ pf,\ fp,\ dg,\ gd$
	$2p^2\rightarrow s^2,\ p^2,\ d^2,\ sd,\ pf,\ dg$
	$3p\,3s\rightarrow ps,\ sp,\ dp,\ pd,\ fd,\ df$
	$3p\,2s\rightarrow ps,\ sp,\ dp,\ pd,\ fd,\ df$
	$2p\,3s\rightarrow ps,\ sp,\ dp,\ pd,\ fd,\ df$
	$2p\,2s\rightarrow ps,\ sp,\ dp,\ pd,\ fd,\ df$
	$3s^2\rightarrow s^2,\ p^2,\ d^2$
	$3s\,2s\rightarrow s^2,\ p^2,\ d^2$
	$2s^2\rightarrow s^2,\ p^2,\ d^2$
$4s$-core	$4s\,3p\rightarrow sp,\ ps,\ pd,\ dp,\ df,\ fd,\ fg,\ gf,\ gh$
	$4s\,2p\rightarrow sp,\ ps,\ pd,\ dp,\ df,\ fd,\ fg,\ gf,\ gh$
	$4s\,3s\rightarrow s^2,\ p^2,\ d^2,\ f^2,\ g^2$
	$4s\,2s\rightarrow s^2,\ p^2,\ d^2,\ f^2,\ g^2$
$4p$-core	$4p\,3p\rightarrow l_1l_2,\ \lvert l_1-1\rvert\le4,\ \lvert l_2-1\rvert\le4$
	$4p\,2p\rightarrow l_1l_2,\ \lvert l_1-1\rvert\le4,\ \lvert l_2-1\rvert\le4$
	$4p\,3s\rightarrow l_1l_2,\ \lvert l_1-1\rvert\le4,\ \lvert l_2-0\rvert\le4$
	$4p\,2s\rightarrow l_1l_2,\ \lvert l_1-1\rvert\le4,\ \lvert l_2-0\rvert\le4$
$3d$-core	$3d\,3p\rightarrow l_1l_2,\ \lvert l_1-2\rvert\le4,\ \lvert l_2-1\rvert\le4$
	$3d\,2p\rightarrow l_1l_2,\ \lvert l_1-2\rvert\le4,\ \lvert l_2-1\rvert\le4$
	$3d\,3s\rightarrow l_1l_2,\ \lvert l_1-2\rvert\le4,\ \lvert l_2-0\rvert\le4$
	$3d\,2s\rightarrow l_1l_2,\ \lvert l_1-2\rvert\le4,\ \lvert l_2-0\rvert\le4$

B. The $4p$ state

All four hyperfine parameters enter for the $4p$ state. Table III shows the results obtained with orbitals created in the Hartree-Fock potential from the Ca^{2+} core. In first order the contact parameter is zero and the orbital, quadrupole, and spin-dipole parameters are all equal and given by the expectation value $\langle r^{-3}\rangle = 1.0231$ a.u. of the $4p$ orbital. The effect of core polarization, evaluated to all orders, is given in the second line in Table III. This effect is the most important correction to the $\langle r^{-3}\rangle$ parameters, increasing them by 25—40%. The largest contributions come from the $3p\rightarrow p$ and $3s\rightarrow s$ excitations.

As for the $4s$ state, the dominating correlation contribution is the modification of the valence orbital to an approximate Brueckner orbital, which increases the expectation value, $\langle r^{-3}\rangle$, by 20% to 1.2232. This value includes, in addition to the third-order diagrams, also fifth-order diagrams like the diagram in Fig. 6(c). It is thus different from the sum of the results in the first and third line of Table III. The most important pair excitations are $4p\,3p\rightarrow sd$, $4p\,3p\rightarrow d^2$, and $4p\,3p\rightarrow p^2$, contributing 0.054, 0.062, and 0.025, respectively, to the $\langle r^{-3}\rangle$ value. Excitations from $4p\,3s$ contribute 0.016 and from $4p\,2p$ 0.013. Excitations involving two core electrons are again very small, contributing only 0.007.

The remaining correlation effects, not taken into account by modifying the valence orbital to an approximate

TABLE III. Contributions to the $\langle r^{-3}\rangle$ parameters for the $4p$ state of Ca^+ using orbitals created in the Hartree-Fock potential from Ca^{2+}. The polarization contributions are evaluated to all orders. All third-order and some higher-order effects are included in the correlation contributions (a.u.).

	Contact	Orbital	Spin-dipole	Quadrupole
$\langle r^{-3}\rangle$	0	1.0231	1.0231	1.0231
Polarization	0.3550	0.2656	0.3033	0.4371
Correlation:				
"Brueckner orbital"	0	0.1943	0.1943	0.1943
Other correlation	−0.1781	−0.0320	−0.0269	−0.0684
Total	0.1769	1.4510	1.4938	1.5861

TABLE IV. Results for the various hyperfine parameters in the $4p$ state of Ca^+ using approximate Brueckner valence orbitals. The pair functions and Brueckner orbital obtained in one iteration were used to create the pair functions in the next iteration. The pair excitations included are shown in Table II (a.u.).

		Pair functions used			
		First order	1 iteration	2 iterations	3 iterations
Contact	$\langle r^{-3}\rangle$	0	0	0	0
	Polarization	0.3890	0.3876	0.3878	0.3878
	Correlation	−0.2010	−0.2007	−0.2036	−0.2037
	Total	0.1880	0.1869	0.1842	0.1841
Orbital	$\langle r^{-3}\rangle$	1.2232	1.2234	1.2258	1.2261
	Polarization	0.2976	0.2969	0.2972	0.2973
	Correlation	−0.0378	−0.0295	−0.0284	−0.0281
	Total	1.4830	1.4908	1.4946	1.4953
Spin-dipole	$\langle r^{-3}\rangle$	1.2232	1.2234	1.2258	1.2261
	Polarization	0.3400	0.3391	0.3398	0.3399
	Correlation	−0.0331	−0.0303	−0.0292	−0.0290
	Total	1.5301	1.5322	1.5364	1.5370
Quadrupole	$\langle r^{-3}\rangle$	1.2232	1.2234	1.2258	1.2261
	Polarization	0.4774	0.4766	0.4770	0.4770
	Correlation	−0.0754	−0.0749	−0.0764	−0.0766
	Total	1.6252	1.6251	1.6264	1.6265

Brueckner orbital, contribute about 3–7% of the first-order value (except for the contact parameter, whose first-order value is zero). Owing to the spin operator in the spin-dipole interaction certain diagrams are forbidden that enter for the quadrupole interaction. The difference in polarization effects for these two parameters, e.g., shows that the direct polarization diagrams [Figs. 2(a)–2(b)] give only about 40% of the exchange polarization diagram [Figs. 2(c)–2(d)] that give identical contributions to the two parameters. The correlation effect (other than the orbital modification) for the quadrupole interaction is more than twice the size of the effect for the spin-dipole interaction, but the magnitude is small. This effect reduces the difference between the two parameters leaving them only 6% different.

Use of the approximate Brueckner valence orbitals in the evaluation of the diagrams changes both the polarization and correlation effects. The new values are given in Table IV, which also shows the convergence in the iteration procedure.

Of more direct experimental interest are the A and B factors. They are related to the $\langle r^{-3}\rangle$ parameters as[3] [C and D have been reevaluated using up-to-date values of α, a_0, and m_p/m_e (Ref. 20)]

$$A(j_<)=C\frac{g_I}{2l+1}\left[(2l+2)\langle r^{-3}\rangle_{01}+\frac{2l+2}{2l-1}\langle r^{-3}\rangle_{12}-\langle r^{-3}\rangle_{10}\right],$$
$$A(j_<)=C\frac{g_I}{2l+1}\left[2l\langle r^{-3}\rangle_{01}-\frac{2l}{2l+3}\langle r^{-3}\rangle_{12}+\langle r^{-3}\rangle_{10}\right], \tag{7}$$

where $C=95.4107(4)$ if A is given in MHz, g_I in nuclear magnetons, and $\langle r^{-3}\rangle$ in atomic units, and

$$B(j_>)=DQ\left[\frac{2l}{2l+3}\langle r^{-3}\rangle_{02}\right],$$
$$B(j_<)=DQ\frac{1}{2l+1}[2(l-1)\langle r^{-3}\rangle_{02}], \tag{8}$$

where $D=234.9649(8)$ if B is given in MHz and Q is given in b (10^{-28} m^2). The values of the A and B factors at different stages are given in Table V.

As for the $4s$ state we have estimated the relativistic effects by performing also relativistic calculations of the core-polarization effect, as described in Ref. 12. The results of these calculations are shown in Table V. For the $4p_{1/2}$ state the HF expectation value and the polarization contribution are both increased by about 4%. The total nonrelativistic contribution from correlation effects is 22.0 MHz and adding 4% to this value as an estimate of relativistic effects leads to a final value, $A(4^2P_{1/2})=-148$ MHz. Although the relativistic effect on the HF values for both the $A(4^2P_{3/2})$ and $B(4^2P_{3/2})$ values is less than one percent, the core-polarization effect is increased by 4% and 2%, respectively. Since it is then difficult to estimate the effect of relativity on the correlation contributions, we add the nonrelativistic correlation contributions to the relativistic results including core polarization to obtain the final values $A(4^2P_{3/2})=-30.9$ MHz and $B(4^2P_{3/2})/Q=155$ MHz/b.

C. The 3d state

The core-polarization and correlation effects are more important for the $3d$ state in Ca^+ than for the $4p$ state, as

TABLE V. A and B factors for the $4p$ states in Ca^+ evaluated with HF orbitals and approximate Brueckner valence orbitals. The values in parentheses are corresponding relativistic results.

	$A(4^2P_{1/2})$ (MHz)	$A(4^2P_{3/2})$ (MHz)	$B(4^2P_{3/2})/Q$ (MHz/b)
Hartree-Fock	−98.0	−19.6	96.2
	(−101.6)	(−19.6)	(97.1)
+ polarization	−121.0	−28.8	137.2
	(−125.4)	(−29.1)	(138.9)
+ correlation	−138.9	−29.7	149.1
Total with "Brueckner orbitals"			
Pair functions used:			
First order	−142.1	−30.4	152.8
1 iteration	−142.5	−30.6	152.7
2 iterations	−143.0	−30.6	152.9
3 iterations	−143.0	−30.6	152.9

can be seen from Table VI. The expectation value is $\langle r^{-3}\rangle = 0.5889$ a.u. if the $3d$ orbital is created in the HF potential from Ca^{2+}. The exchange core polarization gives large negative contributions to the parameters in contrast to the positive values for the $4p$ state and the polarization effects on the quadrupole and spin-dipole parameters are drastically different, with the direct and exchange terms nearly cancelling for the quadrupole interaction. The use of an approximate Brueckner valence orbital increases the $\langle r^{-3}\rangle$ expectation value by about 30%. The largest contributions come from the valence-core excitations $3d\,3p \rightarrow dp$, $+0.11$, and $3d\,3p \rightarrow fd$, $+0.065$, and the core-core excitation $3p^2 \rightarrow d^2$ which contributes -0.054. Also the remaining correlation effects are important, particularly for the spin-dipole parameter, where they amount to about 30% of the first-order value. Again, the use of Brueckner valence orbitals changes both the polarization and the remaining correlation effects. These results are given in Table VII. Owing to the large cancellations, the quadrupole parameter is quite sensitive; the polarization contribution is increased by about 40% and the correlation contribution is reduced by about 40%. The correlation contribution to the contact parameter is increased by about 30%, whereas the contributions to the other parameters undergo less drastic changes.

The A and B factors for the $3d$ states were evaluated using the formulas (7) and (8) and the results are given in Table VIII, showing that the values are very well converged. The changes between the last two lines are very small. The largest change (2%) occurs for the $A(3^2D_{5/2})$ parameter, which is rather sensitive to small changes in the $\langle r^{-3}\rangle$ values due to large cancellations between the orbital and induced contact parameters.

As shown in Table VIII, the relativistic effects lead to a reduction of the expectation value of all the parameters for the $3d$ state in contrast to the situation for the $4s$ and $4p$ states. The relativistic correction factors are quite different for the expectation values and polarization contributions. We are thus not in a position to estimate the relativistic effects on the correlation contributions and choose again to add the nonrelativistic correlation contributions to the relativistic results including core polarization. The final results are $A(3^2D_{3/2}) = -52$ MHz, $B(3^2D_{3/2})/Q = 68$ MHz/b, $A(3^2D_{5/2}) = -5.2$ MHz, and $B(3^2D_{5/2}) = 97$ MHz/b.

The valence $3d$ electron has a relatively large probability of being within the core. Thus it may influence the correlation among the core electrons more than, e.g., a $4s$ or a $4p$ valence electron does. These effects have been neglected and we feel that the omitted effects may not be negligible for the $3d$ state. Table IX shows the Hartree-Fock and Dirac-Fock values for the ionization energies, the nonrelativistic correlation energies obtained from the Brueckner orbital modification procedure, and a comparison with experimental data.[21] For the $4s$ and $4p$ states, the correlation contributions are about 5% larger than the difference between the experimental results and the Dirac-Fock ionization energies, whereas for the $3d$ state the nonrelativistic correlation energy is 14% larger than this difference. Thus the hfs results obtained for the $3d$

TABLE VI. Contributions to the $\langle r^{-3}\rangle$ parameters for the $3d$ state of Ca^+ using orbitals created in the Hartree-Fock potential from Ca^{2+}. The polarization contributions are evaluated to all orders and all third-order effects are included in the correlation contributions (a.u.).

	Contact	Orbital	Spin-dipole	Quadrupole
$\langle r^{-3}\rangle$	0	0.5889	0.5889	0.5889
Polarization	−2.1598	−0.1982	−0.3896	−0.0721
Correlation				
"Brueckner orbital"	0	0.1827	0.1827	0.1827
Other correlation	0.4482	0.1057	0.1903	0.0537
Total	−1.7116	0.6791	0.5723	0.7532

TABLE VII. Results for the various hyperfine parameters in the $3d$ state of Ca^+ obtained with approximate Brueckner valence orbitals. The pair excitations included are shown in Table II (a.u.).

		Pair functions used			
		First order	1 iteration	2 iterations	3 iterations
Contact	$\langle r^{-3}\rangle$	0	0	0	0
	Polarization	−2.3037	−2.2999	−2.3008	−2.3008
	Correlation	0.4648	0.5696	0.5941	0.5939
	Total	−1.8389	−1.7303	−1.7067	−1.7069
Orbital	$\langle r^{-3}\rangle$	0.7725	0.7915	0.7972	0.7987
	Polarization	−0.1985	−0.1969	−0.1965	−0.1964
	Correlation	0.1025	0.1134	0.1223	0.1255
	Total	0.6765	0.7080	0.7230	0.7278
Spin-dipole	$\langle r^{-3}\rangle$	0.7725	0.7915	0.7972	0.7987
	Polarization	−0.3747	−0.3692	−0.3679	−0.3676
	Correlation	0.1904	0.1861	0.1919	0.1928
	Total	0.5882	0.6084	0.6212	0.6239
Quadrupole	$\langle r^{-3}\rangle$	0.7725	0.7915	0.7972	0.7987
	Polarization	−0.0976	−0.0990	−0.0996	−0.0997
	Correlation	0.0564	0.0388	0.0341	0.0321
	Total	0.7313	0.7313	0.7317	0.7311

TABLE VIII. A and B factors for the $3d$ states in Ca^+ evaluated with HF orbitals and approximate Brueckner valence orbitals. The values in parentheses are corresponding relativistic results.

	$A(3^2D_{3/2})$ (MHz)	$A(3^2D_{5/2})$ (MHz)	$B(3^2D_{3/2})/Q$ (MHz/b)	$B(3^2D_{5/2})/Q$ (MHz/b)
Hartree-Fock	−33.8	−14.50	55.4	79.1
	(−33.2)	(−14.14)	(54.5)	(77.2)
+ polarization	−35.2	5.11	48.6	69.4
	(−34.6)	(6.02)	(47.9)	(68.3)
+ correlation	−49.8	−4.87	70.8	101.1
Total with "Brueckner orbitals"				
Pair functions used:				
First order	−50.8	−3.81	68.7	98.2
1 iteration	−51.7	−5.42	68.7	98.2
2 iterations	−52.3	−5.96	68.8	98.2
3 iterations	−52.6	−6.09	68.7	98.2

TABLE IX. Ionization energies for the $4s$, $4p$, and $3d$ states of Ca^+ (a.u.).

		$4p$		$3d$	
	$4s$	$j=\frac{1}{2}$	$j=\frac{3}{2}$	$j=\frac{3}{2}$	$j=\frac{5}{2}$
Hartree-Fock (Ca^{2+})	0.4150	0.3093		0.3331	
Dirac-Fock (Ca^{2+})	0.4167	0.3101	0.3091	0.3310	0.3309
Correlation	0.0207	0.0120		0.0490	
HF + correlation	0.4357	0.3213		0.3821	
DF + correlation	0.4374	0.3221	0.3211	0.3800	0.3799
Experiment (Ref. 21)	0.4363	0.3215	0.3205	0.3741	0.3738
Weighted average		0.3208		0.3739	

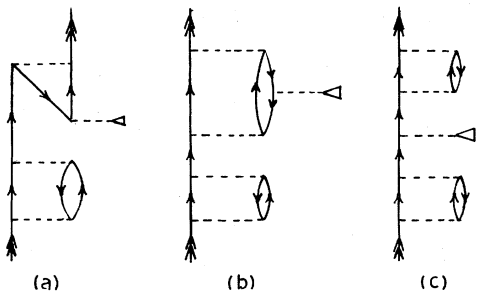

FIG. 6. Examples of higher-order correlation diagrams that are automatically included (a) in the polarization diagram 2(c), (b) in the correlation diagram 4(b), and (c) in the first-order diagram in Fig. 1 when the Hartree-Fock orbitals are replaced by approximate Brueckner orbitals.

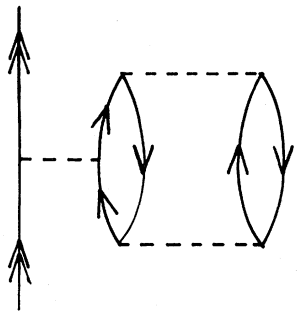

FIG. 7. Example of a third-order energy diagram not included in the present calculations.

state are probably not quite as accurate as the $4s$ and $4p$ results. It should be noted, however, that our hfs calculations include all diagrams up to third order, whereas the calculations of the correlation energies are complete only to second order and we have not yet attempted to include all third-order diagrams for the correlation energies. Figure 7 shows an example of a third-order energy diagram not included.

Although polarization and correlation effects for the $3d$ state in Ca^+ are important, this state is still relatively unperturbed compared to the d states in the isoelectronic system K. A calculation of the hfs for the $5d$ state in K (Ref. 4) showed both polarization and correlation effects comparable to the HF expectation value of $\langle r^{-3} \rangle$. The use of Brueckner orbitals rather than HF orbitals doubled the expectation value and brought changes to the polarization and the remaining correlation effects as large as these effects evaluated with HF orbitals. The different character of the d states in K and Ca^+ is of course evident also from experimental data, e.g., the fine structure of the d states in Ca^+ is normal, whereas it is inverted for K. The quantum defect changes by about one unit in going from Ca^+ to K, while remaining relatively unchanged when going to higher nuclear charges.[22] The difference has been explained[23] by observing that the d orbitals in K are mainly located outside the centrigual barrier in the potential, whereas the nuclear attraction in Ca^+ is sufficiently strong to pull the d orbitals inside the barrier, which is a more stable arrangement.

IV. CONCLUSION

We have used many-body perturbation theory to calculate the hyperfine structure of the $4s$, $4p$, and $3d$ states of Ca^+. These states are relatively well described by a central-field model, but it is still essential to include both polarization and lowest-order correlation effects—these give changes in the A and B factors of up to about 50%. The inclusion of higher-order correlation effects changes the results by only about 2—6% [except for the small $A(3^2D_{5/2})$ factor, which is changed by 25%]. The results obtained appear to have converged well. Relativistic effects were found to be less than about 5% but were quite different for the expectation values and the core polarization for states with $j > \frac{1}{2}$.

The result for the $4s$ state is in agreement with experimental data. No experimental information is yet available for the hyperfine structure of the excited states of Ca^+. However, the calculations performed here are also a part of the evaluation of the hyperfine structure in Ca, which is presented elsewhere.[24]

ACKNOWLEDGMENTS

We have benefited from discussing the results with Professor Ingvar Lindgren and Dr. Leslie Pendrill. We are also indebted to Jean-Louis Heully for performing the calculation of the relativistic core-polarization effects. The work of Kelly *et al.* (Ref. 10) was brought to our attention by Dr. C. W. P. Palmer and Dr. D. N. Stacey at the Clarendon Laboratory, Oxford. This work was financially supported by the Swedish Natural Science Research Council.

*Present address: Department of Physics, University of Virginia, Charlottesville, VA 22901.

[1]S. Forsén and B. Lindman, in *Annual Reports on NMR Spectroscopy,* edited by G. Webb (Academic, New York, 1981), Vol. 11A, p. 183.

[2]S. Garpman, I. Lindgren, J. Lindgren, and J. Morrison, Phys. Rev. A 11, 758 (1975).

[3]S. Garpman, I. Lindgren, J. Lindgren, and J. Morrison, Z. Phys. A 276, 167 (1976).

[4]I. Lindgren, J. Lindgren, and A.-M. Mårtensson, Z. Phys. A 279, 113 (1976); Phys. Rev. A 15, 2123 (1977).

[5]A.-M. Mårtensson, thesis, University of Göteborg (1978).

[6]R. M. Sternheimer, Phys. Rev. 80, 102 (1950); 84, 244 (1951); 86, 315 (1952); 164, 10 (1967); R. M. Sternheimer and R. F. Peierls, Phys. Rev. A 3, 837 (1971); R. M. Sternheimer, *ibid.* 9, 1783 (1974).

[7]See, e.g., M. Vajed-Samii, S. N. Ray, T. P. Das, and J. Andriessen, Phys. Rev. A 20, 1787 (1979).
[8]A.-M. Mårtensson, J. Phys. B 12, 3995 (1979).
[9]I. Lindgren and J. Morrison, in *Atomic Many-Body Theory,* Vol. 13 of *Springer Series in Chemical Physics* (Springer, Berlin, 1982).
[10]F. M. Kelly, H. Kuhn, and A. Pery, Proc. Phys. Soc. London Sect. A 67, 450 (1954).
[11]J. S. M. Harvey, Proc. R. Soc. London Ser. A 285, 581 (1965).
[12]J.-L. Heully and A.-M. Mårtensson-Pendrill, Phys. Scr. 27, 291 (1983); Phys. Rev. A 27, 3332 (1983).
[13]S. Ahmad, J. Andriessen, and T. P. Das, Phys. Rev. A 27, 2790 (1983).
[14]S. Ahmad, J. Andriessen, K. Raughunathan, and T. P. Das, Phys. Rev. A 25, 2923 (1982).
[15]I. Lindgren and S. Salomonson, Phys. Scr. 21, 335 (1980).
[16]H. Lundberg, A.-M. Mårtensson, and S. Svanberg, J. Phys. B 10, 1971 (1977).
[17]C. M. Lederer and V. S. Shirley, *Tables of Isotopes* (Wiley, New York, 1978).
[18]R. Beigang and A. Timmermann, Phys. Rev. A 25, 1496 (1982).
[19]I. I. Sobelman, *Atomic Spectra and Radiative Transitions* (Springer, Berlin, 1979).
[20]Particle Data Group, Rev. Mod. Phys. 52, S33 (1980).
[21]B. Edlén and P. Risberg, Ark. Fys. 10, 553 (1956).
[22]A. R. P. Rau and U. Fano, Phys. Rev. 167, 7 (1968).
[23]D. C. Griffin, K. L. Andrew, and R. D. Cowan, Phys. Rev. 177, 62 (1969).
[24]S. Salomonson, thesis, Chalmers University of Technology, Göteborg (1983); Z. Phys. A (to be published).